Science in China Series G: Physics, Mechanics & Astronomy

www.scichina.com
phys.scichina.com
www.springerlink.com

2Two mode photon bunching effect as witness of quantum criticality in circuit QED

AI Qing[1], WANG YingDan[2], LONG GuiLu[1,3†] & SUN ChangPu[4]

[1] Department of Physics, Tsinghua University, Beijing 100084, China;
[2] Department of Physics, University of Basel, Klingelbergstrasse 82, 4056 Basel, Switzerland;
[3] Tsinghua National Laboratory for Information Science and Technology, Beijing 100084, China;
[4] Institute of Theoretical Physics, Chinese Academy of Sciences, Beijing 100080, China

We suggest a scheme to probe critical phenomena at a quantum phase transition (QPT) using the quantum correlation of two photonic modes simultaneously coupled to a critical system. As an experimentally accessible physical implementation, a circuit QED system is formed by a capacitively coupled Josephson junction qubit array interacting with one superconducting transmission line resonator (TLR). It realizes an Ising chain in the transverse field (ICTF) which interacts with the two magnetic modes propagating in the TLR. We demonstrate that in the vicinity of criticality the originally independent fields tend to display photon bunching effects due to their interaction with the ICTF. Thus, the occurrence of the QPT is reflected by the quantum characteristics of the photonic fields.

quantum phase transition, photon bunching, circuit QED

Inspired by the fast developments of quantum information[T1,2], quantum phase transition (QPT)[3] has renewed much attention in different fields of physics ranging from condensed matter physics to quantum optics[4,5]. Its close relation with entanglement was well explored in spin models[6,7]. It was found that[8] at the quantum critical point the dynamic evolution of a quantum critical system is so extremely sensitive that it can enhance the quantum decoherence of an external system coupled to it. This ultra-sensitivity is characterized by the Loschmidt echo, which is a well-known concept in quantum chaos[9]. In this sense, the quantum-classical transition from a pure state to a mixed one is induced by the quantum criticality of this surrounding system. This discovery motivated a new scheme to probe the QPT by exploring the quantum coherence in the external system and its losses[14].

Moreover, this probing mechanism for quantum criticality was illustrated by a circuit QED architecture[10−12], which was formed by a superconducting Josephson junction qubit array interacting with a one-dimensional superconducting transmission line resonator (TLR)[13]. The superconducting qubit array was modeled as an Ising chain in the transverse field (ICTF). This investigation showed that the QPT phenomenon in the superconducting qubit array was evidently revealed by the correlation spectrum of TLR output. Though this mechanism for the circuit QED system has not been experimentally tested, an NMR simulation experiment[14] has been carried out to demonstrate the QPT-like phenomenon (energy level crossing) as predicted in ref. [8] by exploring the increased sensibility of the quantum system to perturbation when it is close to a critical point.

For the above circuit QED architecture to demon-

Received May 11, 2009; accepted June 11, 2009
doi: 10.1007/s11433-009-0274-z
†Corresponding author (email: gllong@mail.tsinghua.edu.cn, gllong@tsinghua.edu.cn)
Supported by the National Basic Research Program of China (Grant No. 2006CB921106), the National Natural Science Foundation of China (Grant No. 10874098) and the ECIST-FET Project EuroSQUIP, the Swiss SNF, and the NCCR Nanoscience
Contributed by LONG GuiLu

Citation: Ai Q, Wang Y D, Long G L, et al. Two mode photon bunching effect as witness of quantum criticality in circuit QED. Sci China Ser G, 2009, 52(12): 1898-1905, doi: 10.1007/s11433-009-0274-z

strate the probing of the QPT, we notice that with two modes simultaneously coupled to a charge qubit, their squeezing effect was investigated theoretically[15]. Here, we consider the full application of quantum optics approach[16] in the detection of the QPT by considering the higher order quantum coherence. To this end, we consider that a Josephson junction qubit array modeled as the ICTF simultaneously couples to two modes propagating in the TLR. Since all quasi-spins homogeneously interact with the fields, we can obtain the first (second) order correlation function of the two fields. According to our calculation, the second order quantum coherence is given in terms of the decoherence factor of the ICTF. As proven in Appendix A, the norm of the decoherence factor decreases exceptionally when the ICTF is at the critical point. Therefore, the photon bunching effect occurs since the second order quantum coherence of the steady state is smaller compared with its initial value. And these results show genetic characteristics of the quantum spin chain in the vicinity of the critical point.

The paper is structured as follows. The next section describes the ICTF formed by a capacitively coupled Josephson junction qubit array is coupled to two independent fields propagating in the TLR. Then the detection scheme of the QPT and the correlation functions of two mode fields are given in Sec 2. A brief summary is given in Sec 3. Furthermore, in addition to the main body of the paper, Appendix A presents the details about the calculation of the decoherence factor. Since the theoretical deduction is based on the rotating wave approximation (RWA), its validity has been proven in Appendix B.

1 Circuit QED based setup for probing quantum criticality

We consider a circuit QED system illustrated in Figure 1. N Cooper pair boxes (CPBs) are capacitively coupled one by one. Formed by a superconducting island connected with two Josephson junctions, each CPB is a direct current superconducting quantum interference device (dcSQUID). Since the magnetic flux Φ_x threading the dcSQUID is tunable, the effective Josephson tunnelling energy can be varied. With proper bias voltage, the CPB behaves as a qubit near the degeneracy point and then Josephson junction qubit array becomes a spin chain with N 1/2-spins. When the coupling capacitance C_m between two CPBs is much smaller than the total one

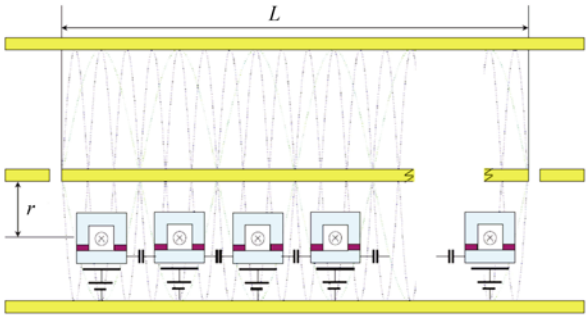

Figure 1 Schematic diagram of superconducting Ising chain interacting with two largely detuned modes ($\uparrow_1$=3 $\uparrow_2$) individually transmitted in the TLR. Since the CPBs are located at the antinodes of both modes, i.e, $x_j=(j-1/2)\pi v/\omega_2$, they only interact with the magnetic fields.

C_Σ to each CPB, the high order terms in Hamiltonian can be neglected and only the nearest neighbor interaction is considered. Then the qubit array can be approximated as an ICTF with ref. [14]:

$$H_0 = B\sum_{j=1}^{N} \lambda\sigma_j^x + \sigma_j^z\sigma_{j+1}^z, \tag{1}$$

where $\sigma^x = -|0\rangle\langle 1| - |1\rangle\langle 0|$ and $\sigma^z = |0\rangle\langle 0| - |1\rangle\langle 1|$ with $|n\rangle$ being the state of n extra Cooper pairs on the superconducting island, $\lambda = B_x / B$ and $B = e^2 C_m / C_\Sigma^2$, $B_x = E_J \cos(\pi\Phi_x / \Phi_0)$ is the Josephson energy of each CPB with E_J the Josephson energy of single junction, $\Phi_0 = h/2e$ the flux quantum.

In a one dimensional TLR, the electric current and voltage at the position x are given as

$$I(x,t) = \sum_k \sqrt{\frac{\hbar\omega_k}{Ll}}(a_k^\dagger + a_k)\sin\frac{k\pi x}{L}, \tag{2}$$

$$V(x,t) = -i\sum_k \sqrt{\frac{\hbar\omega_k}{Lc}}(a_k^\dagger - a_k)\cos\frac{k\pi x}{L}, \tag{3}$$

where $a_k^\dagger$ is the creation operator with frequency ω_k, L the length of TLR, l and c the induction and capacitance of per unit length of TLR respectively, k positive integer. Therefore, a CPB located at the antinode is only coupled to the magnetic field since the electric field vanishes. According to Ampere's circuital law, when a dc SQUID loop is placed at a distance r with respect to the center of the TLR, the quantum magnetic flux that threads it is

$$\Phi_q(x) = \frac{\mu_0 IS}{2\pi r} = \frac{\mu_0 S}{2\pi r}\sum_k \sqrt{\frac{\hbar\omega_k}{Lc}}(a_k^\dagger + a_k)\sin\frac{k\pi x}{L}, \tag{4}$$

where μ_0 is the vacuum magnetic permeability, S the

area of dc SQUID loop. The interaction between the CPBs and the magnetic field is written as

$$H_{\Phi} = E_{\mathrm{J}} \sum_j \cos \frac{\pi \Phi_{\mathrm{q}}(x_j)}{\Phi_0} \sigma_j^x. \tag{5}$$

In our consideration, two independent modes with frequencies $\omega_1 = 3\omega_2$ are propagating in the TLR. All the CPBs are placed the antinodes of the both modes with the positions

$$x_j = \frac{\left(j - \frac{1}{2}\right)\pi v}{\omega_2}, \tag{6}$$

where

$$\omega_2 = \frac{\pi v L}{M}, \tag{7}$$

j and M are positive integers, v the velocity of the light. Since $\Phi_{\mathrm{q}} \ll \Phi_0$, under the RWA[16], the interaction Hamiltonian is approximated to the second order,

$$H_{\Phi} = E_{\mathrm{J}} \sum_j \left\{1 - \frac{1}{2}[\eta_1^2(2a_1^+ a_1 + 1) + \eta_2^2(2a_2^+ a_2 + 1)]\right\}\sigma_j^x, \tag{8}$$

where the coupling constants between the two modes and individual spins are

$$\eta_k = \frac{\pi \mu_0 S}{2\pi r \Phi_0}\sqrt{\frac{\hbar \omega_k}{Ll}}. \tag{9}$$

For realistic parameters, $C_{\Sigma} = 600$ aF, $C_m = 30$ aF, $L_0 = 1$ cm, $S_0 = 10$ μm^2, $r = 1$ μm, $N = 500$, $E_{\mathrm{J}} = 13$ GHz, we have $B = 1.6$ GHz, $\omega_2 \approx 120$ GHz, $\eta_1 = \sqrt{3}\eta_2$, and $\eta_2 \approx 0.1$[14].

Thus, the total Hamiltonian is written as

$$\begin{aligned} H = {} & \omega_1 a_1^+ a_1 + \omega_2 a_2^+ a_2 \\ & + E_{\mathrm{J}} \sum_j \left\{1 - \frac{1}{2}[\eta_1^2(2a_1^+ a_1 + 1) + \eta_2^2(2a_2^+ a_2 + 1)]\right\}\sigma_j^x \\ & + \frac{e^2 C_{\Sigma}}{C_m^2} \sum_j \sigma_j^z \sigma_j^z. \end{aligned} \tag{10}$$

The validity of the RWA is proven in Appendix B. Furthermore, since there is no energy exchange between the fields and the ICTF, the total Hamiltonian can be decomposed into invariant subspaces with respect to the Fock state of the fields,

$$H = \sum_{m,n} H^{(m,n)} |m\rangle|n\rangle\langle n|\langle m|, \tag{11}$$

where

$$H^{(m,n)} = B\sum_{j=1}^{N} \lambda_{m,n}\sigma_j^x + \sigma_j^z \sigma_{j+1}^z, \tag{12}$$

with $\lambda_{m,n} = E_{\mathrm{J}}[1 - \eta_1^2(m + 1/2) + \eta_2^2(n + 1/2)]/B$.

Generally speaking, the Hamiltonian of ICTF H_0 is transformed into a quadratic Fermion form with Jordan-Wigner transformation[3]

$$c_j = \exp\left(\pi \mathrm{i} \sum_{k=1}^{j-1} \sigma_k^z\right)\sigma_j^+. \tag{13}$$

Then, by introducing quasi-particle operator[17]

$$\gamma_k = \sum_{j=1}^{N} \frac{\mathrm{e}^{-\mathrm{i}kj}}{\sqrt{N}}\left(\cos\frac{\theta_k}{2} c_j - \mathrm{i}\sin\frac{\theta_k}{2} c_j^{\dagger}\right) \tag{14}$$

with

$$\theta_k(\lambda) = \tan^{-1}\frac{\sin k}{\lambda - \cos k}, \tag{15}$$

H_0 is diagonalized as

$$H_0 = \sum_k \varepsilon_k \left(\gamma_k^{\dagger}\gamma_k - \frac{1}{2}\right) \tag{16}$$

with single particle spectrum being

$$\varepsilon_k(\lambda) = 2B\sqrt{1 + \lambda^2 - 2\lambda\cos k}. \tag{17}$$

And the ground state $|G\rangle$ corresponds to no quasiparticle excitation at all.

2 Photon bunching effect

Followed by a series of advances, i.e., resonance fluorescence, the Hanbury-Brown-Twiss experiment[18] reopens philosophical debate about photons[19] and sets itself as the milestone in the development of quantum optics. All these experimental phenomena are associated with the correlation functions of the field. Here, we consider it as the method to detect the QPT since the two fields propagating in the TLR interact with the quasi-spins respectively.

First of all, we define an operator

$$A = a_1 + \mathrm{i}a_2. \tag{18}$$

The first order correlation function is written as $\langle A^{\dagger}(t)A\rangle$. Here, the bracket $\langle\cdots\rangle$ denotes average over the initial state, with the Ising chain in the ground state $|G\rangle$ and the two fields being in arbitrary pure states $\sum_m c_m|m\rangle$ and $\sum_n d_n|n\rangle$ respectively. Therefore,

$$\begin{aligned} \langle A^{\dagger}(t)A\rangle = {} & \sum_{m,n} |c_m|^2 |d_n|^2 (m r_{m-1,n}^{(m,n)} + n r_{m,n-1}^{(m,n)}) \\ & - \mathrm{i} c_{m-1}^* c_m d_{n+1}^* d_n \sqrt{m(n+1)}\, r_{m-1,n}^{(m-1,n+1)} \\ & + \mathrm{i} c_{m+1}^* c_m d_{n-1}^* d_n \sqrt{(m+1)n}\, r_{m,n-1}^{(m+1,n-1)}, \end{aligned} \tag{19}$$

where

$$r_{m',n'}^{(m,n)}(t)=\left\langle G\left|\mathrm{e}^{\mathrm{i}H^{(m,n)}t}\mathrm{e}^{-\mathrm{i}H^{(m',n')}t}\right|G\right\rangle \tag{20}$$

is the decoherence factor[8] which measures the overlap of the ground state evolving under two different Hamiltonians. Details about its calculation is presented in Appendix A. In ref. [12], it was discovered that for the same amount of environment dissipation the first order correlation function of the single mode decreased more rapidly in the vicinity of the QPT than in the other region. Moreover, the second order correlation function is analytically written as

$$\begin{aligned}\left\langle A^{\dagger}A^{\dagger}(t)A(t)A\right\rangle=&\sum_{m,n}\left|c_m\right|^2\left|d_n\right|^2[(m+n)(m+n-1)\\&+mnr_{m,n-1}^{(m-1,n)}\mathrm{e}^{-\mathrm{i}(\omega_1-\omega_2)t}+mnr_{m-1,n}^{(m,n-1)}\mathrm{e}^{\mathrm{i}(\omega_1-\omega_2)t}]\\&+\mathrm{i}c_{m+1}^{*}c_m d_{n-1}^{*}d_n\{(m+n-1)\sqrt{(m+1)n}\\&+[m\sqrt{(m+1)n}r_{m-1,n}^{(m,n-1)}\\&+(n-1)\sqrt{(m+1)n}r_{m,n-1}^{(m+1,n-2)}]\mathrm{e}^{\mathrm{i}(\omega_1-\omega_2)t}\}\\&-\mathrm{i}c_{m-1}^{*}c_m d_{n+1}^{*}d_n\{(m+n-1)\sqrt{m(n+1)}\\&+[(m-1)\sqrt{m(n+1)}r_{m-1,n}^{(m-2,n+1)}\\&+n\sqrt{m(n+1)}r_{m,n-1}^{(m-1,n)}]\mathrm{e}^{-\mathrm{i}(\omega_1-\omega_2)t}\}\\&-c_{m+2}^{*}c_m d_{n-2}^{*}d_n\sqrt{(m+2)(m+1)n(n-1)}r_{m,n-1}^{(m+1,n-2)}\mathrm{e}^{\mathrm{i}(\omega_1-\omega_2)t}\\&-c_{m-2}^{*}c_m d_{n+2}^{*}d_n\sqrt{(n+2)(n+1)m(m-1)}r_{m-1,n}^{(m-2,n+1)}\mathrm{e}^{-\mathrm{i}(\omega_1-\omega_2)t}.\end{aligned} \tag{21}$$

Thus, for the fields initially in the state $(|0\rangle+|1\rangle)/\sqrt{2}$, it is straightforward to obtain

$$\left\langle A^{\dagger}A^{\dagger}(t)A(t)A\right\rangle=\frac{1}{2}[1+\mathrm{Re}(r_{0,1}^{(1,0)}\mathrm{e}^{\mathrm{i}(\omega_1-\omega_2)t})], \tag{22}$$

where Re(x) means the real part of x.

As proven in Appendix A, in the vicinity of the QPT, the square of the norm of $r_{0,1}^{(1,0)}(t)$ decreases more rapidly than exponential, i.e,

$$\left|r_{0,1}^{(1,0)}(t)\right|^2\leqslant\mathrm{e}^{-\gamma t^2}. \tag{23}$$

where $\gamma=4B^2(\lambda_{1,0}-\lambda_{0,1})^2E(k_c)/(\lambda_{0,1}-1)^2$, $E(k_c)=4\pi^2N_c(N_c+1)(2N_c+1)/6N^2$ with N_c being the nearest integer to $Nk_c/2\pi$.

It can be seen that there is a vanishing numerator $E(k_c)$ as $N\to\infty$. It is doubtful that the exponential decay of $\left|r_{0,1}^{(1,0)}(t)\right|^2$ can truly occur since the QPT takes place in the thermodynamical limit. However, as the size of the ICTF gets larger, we can adjust the parameter $\lambda_{0,1}$ closer to the critical point to make the denominator $(\lambda_{0,1}-1)^2$ small enough. In that case, γ stays as a constant and the $\left|r_{0,1}^{(1,0)}(t)\right|^2$ decreases exponentially with time. For a real system, N is finite for the demonstration of the QPT. To test the validity of the above analysis, we resort to numerical simulation. In Figure 2, we plot the evolution of $\left|r_{0,1}^{(1,0)}(t)\right|^2$ according to eq. (a9). It can be seen that despite some oscillations $\left|r_{0,1}^{(1,0)}(t)\right|^2$ decays exceptionally at the critical point.

According to ref. [16], the photon bunching and antibunching effects are associated with the second order degree of coherence

$$g^{(2)}(t)=\frac{\left\langle A^{\dagger}A^{\dagger}(t)A(t)A\right\rangle}{\left\langle A^{\dagger}A\right\rangle\left\langle A^{\dagger}(t)A(t)\right\rangle}, \tag{24}$$

which is the normalized second order correlation function of the fields. For the fields both in the state $(|0\rangle+|1\rangle)/\sqrt{2}$, the second order degree of coherence is simplified as

$$g^{(2)}(t)=\frac{1}{2}\frac{1+\mathrm{Re}(r_{0,1}^{(1,0)}\mathrm{e}^{\mathrm{i}(\omega_1-\omega_2)t})}{1-\mathrm{Im}(r_{0,1}^{(1,0)}\mathrm{e}^{\mathrm{i}(\omega_1-\omega_2)t})}$$

with Im(x) being the image part of x.

Since the norm of the decoherence factor decreases exponentially at the critical point, it is obvious that both the real and image parts of $r_{0,1}^{(1,0)}(t)\mathrm{e}^{\mathrm{i}(\omega_1-\omega_2)t}$ will vanish in that limit. As a consequence, we expect the second order degree of coherence to be less than unity in the steady state, i.e., $g^{(2)}(t)=1/2<g^{(2)}(0)=1$. Generally speaking, classical fields, such as thermal light and coherent light, prefer to distribute themselves in bunches rather than at random. They exhibit less correlation for time longer than the correlation time. This is the so-called bunching effect[16]. On the contrary, in certain quantum optical systems, fewer quantum photons are detected close together than further apart. And the photon antibunching observed in fluorescent light from a two-level atom[19] is of such kind. Here, since the two fields involved are two independent modes, we expect photons to be neither bunching nor antibunching, regardless of quantum mechanical fields or classical fields. However, as shown in Figure 3, when the Ising chain is at the critical point, the two independent fields initially

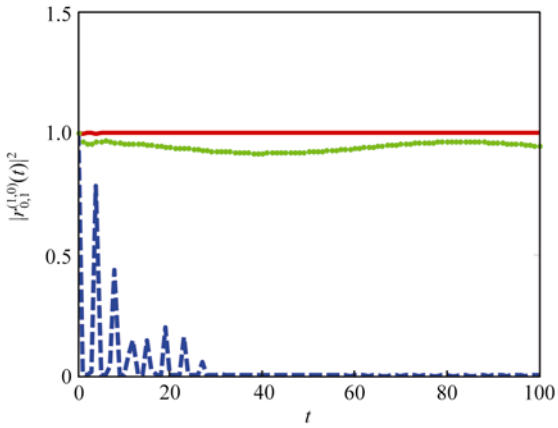

Figure 2 The decoherence factor $\left|r_{0,1}^{(1,0)}(t)\right|^2$ for both fields in $(|0\rangle+|1\rangle)/\sqrt{2}$ is plotted with $\lambda = 8000$. The blue dashed line for $\lambda = 1$, the red solid line for $\lambda = 0.1$, and the green dotted line for $\lambda = 2$. In all figures, t is in units of $1/B$.

in $(|0\rangle+|1\rangle)/\sqrt{2}$ display the photon bunching effect. Further witness is also demonstrated in Figures 4(a)—(c). It can also be proven that $g^{(2)}(t) < g^{(2)}(0)$ for both fields in the coherent state $|\alpha\rangle$ which is not shown here. In Figure 4(d), we plot the time evolution of the second order of coherence for this case. Here, we remark that the two initially independent quantum fields display the classical effect due to their common interaction with the quantum critical system. As illustrated in eq. (20), two initially identical states evolve under two slightly different Hamiltonians. Although the differences between these Hamiltonians are tiny, their evolution trajectories are quite distinct in the vicinity of the QPT. Thus, this slight difference leads to the exponential de-

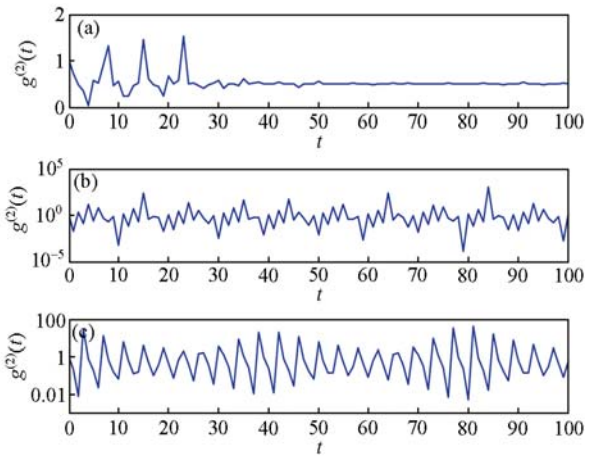

Figure 3 The second order degree of coherence $g^{(2)}(t)$ for $\lambda = 4000$ and $(|0\rangle+|1\rangle)/\sqrt{2}$ is plotted with (a) $\lambda = 1$, (b) $\lambda = 0.1$, (c) $\lambda = 2$.

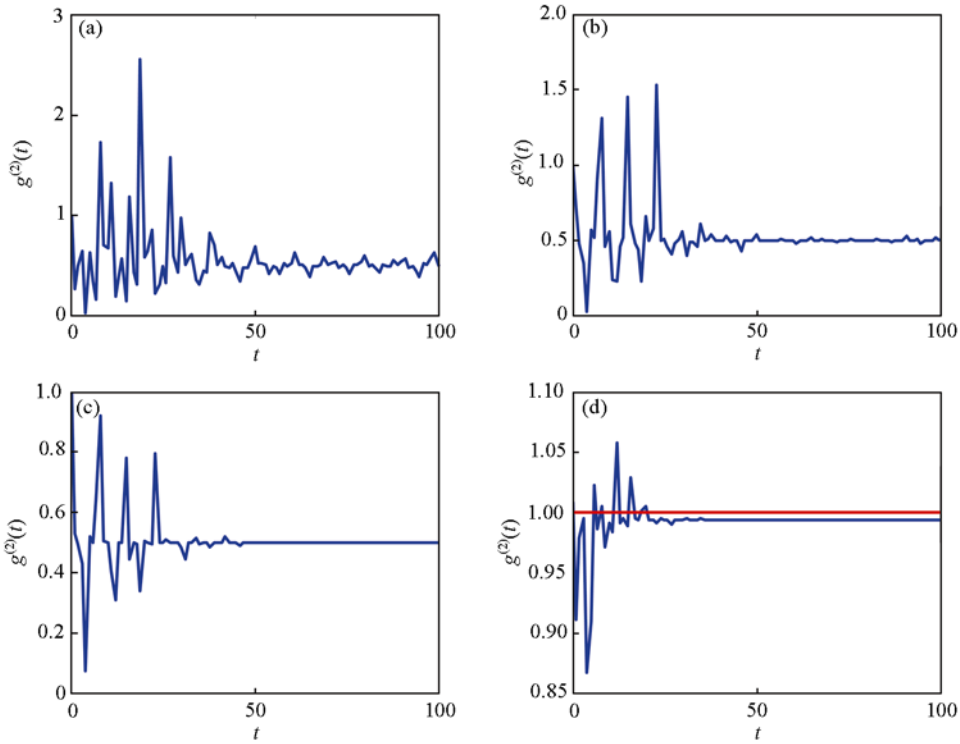

Figure 4 The second order degree of coherence $g^{(2)}(t)$ is plotted at the critical point for $(|0\rangle+|1\rangle)/\sqrt{2}$ with (a) $N = 2000$, (b) $N = 4000$, (c) $N = 8000$. For (d), both fields are in the coherent $|\alpha\rangle$ with $\alpha = 1$ and $N = 8000$. Note that at the steady state $g^{(2)}(t)$ is a little smaller than its original value 1 as indicated by the red horizontal line.

cay of their decoherence factor. It can be understood as a signature of quantum chaos[8].

Furthermore, for the parameters mentioned after eq. (9) and $N_c = N/10$, both the real and imaginary parts of $r_{0,1}^{(1,0)}(t)\mathrm{e}^{\mathrm{i}(\omega_1-\omega_2)t}$ decay with a rate of the order $\sqrt{\gamma} \approx$ 2.5 GHz. Since the dissipation rate of the first excitation mode is about 6.3 MHz[10], we can neglect the influence due to the dissipation of TLR.

3 Conclusion and remark

To conclude, we have explored the possibility to probe quantum criticality in the ICTF by detecting the higher order quantum coherence of the two modes of cavity fields coupled to the spins. We suggest a physical implementation of this theoretical scheme based on a circuit QED system where the capacitively coupled CPBs are coupled to the TLR. Situated at the antinodes of both modes propagating in the TLR, CPBs are only coupled to the magnetic fields. In a heuristic way, we show the decoherence factor decays exponentially with time in the vicinity of the critical point. The second order of coherence is smaller than the one at the steady state. Thus, the two initially independent modes demonstrate photon bunching effect. This can serve as a witness of the QPT.

On the other hand, we have not investigated decoherence originated from the dissipation of the CPBs. We notice that in a recent work[20], the QPT in the dissipative random transverse-field Ising chain was investigated. It was discovered that the quantum critical point was ruined by the interplay between quantum fluctuations and Ohmic dissipation. Further exploration may be done when such kind of effect is considered.

Appendix A Decoherence factor

Following the method introduced in ref. [14], the decoherence factor $r_{m',n'}^{(m,n)}(t)$ can be calculated in the following way.

By introducing the spin-1 pseudospin operators[21]

$$\begin{aligned} s_{xk} &= \mathrm{i}(\gamma_{-k}\gamma_k + \gamma_{-k}^{\dagger}\gamma_k^{\dagger}), \\ s_{yk} &= \gamma_{-k}^{\dagger}\gamma_k^{\dagger} - \gamma_{-k}\gamma_k, \\ s_{zk} &= \gamma_k^{\dagger}\gamma_k + \gamma_{-k}^{\dagger}\gamma_{-k} - 1, \end{aligned} \tag{a1}$$

the Hamiltonian H_0 can also be rewritten as

$$H_0 = \sum_{k>0} \varepsilon_k s_{zk}. \tag{a2}$$

Because there is no energy exchange between the two modes and the qubit array, the total Hamiltonian can be decomposed into invariant subspaces with respect to the Fock state of the fields, i.e., $H = \sum_{m,n} H^{(m,n)} |m\rangle|n\rangle\langle n|\langle m|$, where

$$H^{(m,n)} = B\sum_{j=1}^{N} \lambda_{m,n}\sigma_j^x + \sigma_j^z\sigma_{j+1}^z. \tag{a3}$$

With the pseudospin operators, we can also diagonalize the Hamiltonian as

$$H^{(m,n)} = \sum_{k>0} \varepsilon_k^{(m,n)} s_{zk}^{(m,n)}, \tag{a4}$$

where $s_{zk}^{(m,n)} = s_{zk}\cos 2\alpha_k^{(m,n)} + s_{xk}\sin 2\alpha_k^{(m,n)}$, with $2\alpha_k^{(m,n)} = \theta_k^{(m,n)} - \theta_k$, $\varepsilon_k^{(m,n)} = \varepsilon_k(\lambda_{m,n})$, $\theta_k^{(m,n)} = \theta_k(\lambda_{m,n})$.

Therefore, the ground state of H_0 is the product state of all pseudospins down $|-\rangle_k$,

$$\begin{aligned} |G\rangle &= \prod_{k>0}^{\otimes} |-\rangle_k \\ &= \prod_{k>0}^{\otimes} [\cos\alpha_k^{(m,n)} |-\rangle_k^{(m,n)} + s_{xk}\sin\alpha_k^{(m,n)} |+\rangle_k^{(m,n)}] \end{aligned} \tag{a5}$$

with $|\pm\rangle_k^{(m,n)}$ being the eigen states of $s_{zk}^{(m,n)}$.

Since

$$\begin{aligned} {}_k^{(m,n)}\langle \pm | \pm \rangle_{k'}^{(m',n')} &= \delta_{kk'}\cos(\alpha_k^{(m,n)} - \alpha_k^{(m',n')}), \\ {}_k^{(m,n)}\langle + | - \rangle_{k'}^{(m',n')} &= \delta_{kk'}\sin(\alpha_k^{(m,n)} - \alpha_k^{(m',n')}), \\ {}_k^{(m,n)}\langle - | + \rangle_{k'}^{(m',n')} &= -\delta_{kk'}\sin(\alpha_k^{(m,n)} - \alpha_k^{(m',n')}), \end{aligned} \tag{a6}$$

we have

$$r_{m',n'}^{(m,n)}(t) = \prod_{k>0} \sum_{a_k,b_k=\pm} C_{a_k,b_k,k}^{(m,n,m',n')} \mathrm{e}^{\mathrm{i}(a_k\varepsilon_k^{(m,n)} + b_k\varepsilon_k^{(m',n')})t} \tag{a7}$$

with

$$\begin{aligned} C_{+,+,k}^{(m,n,m',n')} &= \sin\alpha_k^{(m,n)}\cos\alpha_k^{(m',n')}\sin(\alpha_k^{(m,n)} - \alpha_k^{(m',n')}), \\ C_{-,-,k}^{(m,n,m',n')} &= -\cos\alpha_k^{(m,n)}\sin\alpha_k^{(m',n')}\sin(\alpha_k^{(m,n)} - \alpha_k^{(m',n')}), \\ C_{+,-,k}^{(m,n,m',n')} &= \sin\alpha_k^{(m,n)}\sin\alpha_k^{(m',n')}\cos(\alpha_k^{(m,n)} - \alpha_k^{(m',n')}), \\ C_{-,+,k}^{(m,n,m',n')} &= \cos\alpha_k^{(m,n)}\cos\alpha_k^{(m',n')}\cos(\alpha_k^{(m,n)} - \alpha_k^{(m',n')}). \end{aligned} \tag{a8}$$

For a heuristic analysis, we obtain the short time behavior of $\left|r_{0,1}^{(1,0)}(t)\right|^2$ at the critical point.

$$\begin{aligned} \left|r_{0,1}^{(1,0)}(t)\right|^2 &= \prod_{k>0} F_k \\ &\leqslant \prod_{k>0}^{k_c} [\sin^2(\alpha_k^{(1,0)} - \alpha_k^{(0,1)})\cos(\varepsilon_k^{(1,0)} + \varepsilon_k^{(0,1)})t \end{aligned}$$

$$+\cos^2(\alpha_k^{(1,0)}-\alpha_k^{(0,1)})\cos(\varepsilon_k^{(1,0)}-\varepsilon_k^{(0,1)})t]$$
$$+[\sin(\alpha_k^{(1,0)}+\alpha_k^{(0,1)})\sin(\alpha_k^{(1,0)}-\alpha_k^{(0,1)})\cos(\varepsilon_k^{(1,0)}+\varepsilon_k^{(0,1)})t$$
$$-\cos(\alpha_k^{(1,0)}+\alpha_k^{(0,1)})\cos(\alpha_k^{(1,0)}-\alpha_k^{(0,1)})\sin(\varepsilon_k^{(1,0)}+\varepsilon_k^{(0,1)})t]^2. \quad (a9)$$

Since all factors F_k of $\left|r_{0,1}^{(1,0)}(t)\right|^2$ have a norm less than unity, we may expect the $\left|r_{0,1}^{(1,0)}(t)\right|^2$ to vanish under certain conditions. Here, we set a cutoff frequency k_c and hence we have $\left|r_{0,1}^{(1,0)}(t)\right|^2 \leqslant \prod_{k>0}^{k_c} F_k$. For small k, we have

$$\varepsilon_k^{(1,0)} \approx 2B\left|1-\lambda_{1,0}\right|,$$
$$\varepsilon_k^{(0,1)} \approx 2B\left|1-\lambda_{0,1}\right|,$$
$$\theta_k(\lambda) \approx \frac{k}{\lambda-1},$$
$$\alpha_k^{(1,0)} \approx \frac{1}{2}\left(\frac{k}{\lambda_{1,0}-1}-\frac{k}{\lambda_{0,0}-1}\right),$$
$$\alpha_k^{(0,1)} \approx \frac{1}{2}\left(\frac{k}{\lambda_{0,1}-1}-\frac{k}{\lambda_{0,0}-1}\right).$$

To the second order of $\alpha_k^{(1,0)} \pm \alpha_k^{(0,1)}$, we obtain

$$\left|r_{0,1}^{(1,0)}(t)\right|^2 \leqslant \prod_{k>0}^{k_c}[1-2(\alpha_k^{(1,0)}-\alpha_k^{(0,1)})^2]\cos^2(\varepsilon_k^{(1,0)}-\varepsilon_k^{(0,1)})t$$
$$+2(\alpha_k^{(1,0)}-\alpha_k^{(0,1)})^2\cos(\varepsilon_k^{(1,0)}+\varepsilon_k^{(0,1)})t\cos(\varepsilon_k^{(1,0)}-\varepsilon_k^{(0,1)})t$$
$$+[1-2(\alpha_k^{(1,0)})^2-(\alpha_k^{(0,1)})^2]\sin^2(\varepsilon_k^{(1,0)}-\varepsilon_k^{(0,1)})t$$
$$-2[(\alpha_k^{(1,0)})^2-(\alpha_k^{(0,1)})^2]\sin(\varepsilon_k^{(1,0)}+\varepsilon_k^{(0,1)})t$$
$$\times\sin(\varepsilon_k^{(1,0)}-\varepsilon_k^{(0,1)})t.$$

Since $0 \approx \varepsilon_k^{(1,0)}-\varepsilon_k^{(0,1)} \ll \varepsilon_k^{(1,0)}+\varepsilon_k^{(0,1)} = 2\varepsilon_k^{(1,0)}$, we focus on the short time behavior and therefore

$$\left|r_{0,1}^{(1,0)}(t)\right|^2 \leqslant \prod_{k>0}^{k_c}[1-2(\alpha_k^{(1,0)}-\alpha_k^{(0,1)})^2]$$
$$+2(\alpha_k^{(1,0)}-\alpha_k^{(0,1)})^2\cos(2\varepsilon_k^{(1,0)}t)$$
$$=\prod_{k>0}^{k_c}1-2(\alpha_k^{(1,0)}-\alpha_k^{(0,1)})^2\sin(2\varepsilon_k^{(1,0)}t)$$
$$=\prod_{k>0}^{k_c}1-2\frac{k^2(\lambda_{1,0}-\lambda_{0,1})^2}{(1-\lambda_{0,1})^2(1-\lambda_{1,0})^2}\sin\left(2Bt\left|1-\lambda_{1,0}\right|\right).$$

As $\lambda_{1,0} \to 1$, we have

$$\left|r_{0,1}^{(1,0)}(t)\right|^2 \leqslant \mathrm{e}^{-\gamma t^2},$$

where $\gamma = 4B^2(\lambda_{1,0}-\lambda_{0,1})^2E(k_c)/(\lambda_{0,1}-1)^2$, $E(k_c) = 4\pi^2N_c(N_c+1)(2N_c+1)/6N^2$ with N_c being the nearest integer to $Nk_c/2\pi$.

Appendix B Validity of rotating wave approximation

In this section, the validity of the RWA is proven for its application in obtaining eq. (10).

The original Hamiltonian before the RWA is

$$H = E_J\sum_j\cos[\eta_1(a_1^+ + a_1)+\eta_2(a_2^+ + a_2)]\sigma_j^x$$
$$+\frac{\mathrm{e}^2C_m}{C_\Sigma^2}\sum_j\sigma_j^z\sigma_{j+1}^z\omega_1a_1^+a_1+\omega_2a_2^+a_2. \quad (b1)$$

Since $\eta_{1,2} \ll 1$, the Hamiltonian is approximated to the second order as

$$H = \omega_1a_1^+a_1+\omega_2a_2^+a_2$$
$$+E_J\sum_j\left\{1-\frac{1}{2}[\eta_1(a_1^+ + a_1)+\eta_2(a_2^+ + a_2)]^2\right\}\sigma_j^x$$
$$+\frac{\mathrm{e}^2C_\Sigma}{C_m^2}\sum_j\sigma_j^z\sigma_j^z. \quad (b2)$$

In the interaction picture with respect to $H_0' = \omega_1a_1^+a_1 + \omega_2a_2^+a_2$,

$$H = E_J\sum_j\left\{1-\frac{1}{2}[\eta_1^2(2a_1^+a_1+1+a_1^{+2}\mathrm{e}^{\mathrm{i}2\omega_1t}+h.c.)\right.$$
$$+\eta_2^2(2a_2^+a_2+1+a_2^{+2}\mathrm{e}^{\mathrm{i}2\omega_2t}+h.c.)$$
$$\left.+2\eta_1\eta_2(a_1^+a_2^+\mathrm{e}^{\mathrm{i}(\omega_1+\omega_2)t}+a_1^+a_2\mathrm{e}^{\mathrm{i}(\omega_1-\omega_2)t}+h.c.)]\right\}\sigma_j^x$$
$$+\frac{\mathrm{e}^2C_\Sigma}{C_m^2}\sum_j\sigma_j^z\sigma_j^z. \quad (b3)$$

Since the system evolution is determined by the time-dependent Schrödinger equation

$$H\left|\psi(t)\right\rangle = \mathrm{i}\hbar\frac{\partial}{\partial t}\left|\psi(t)\right\rangle, \quad (b4)$$

its solution is formally written as

$$\int_0^t H\left|\psi(t')\right\rangle\mathrm{d}t' = \mathrm{i}\hbar[\left|\psi(t)\right\rangle-\left|\psi(0)\right\rangle]. \quad (b5)$$

As long as $2\omega_1 \gg E_J\eta_1^2/2$, $2\omega_2 \gg E_J\eta_2^2/2$, $\omega_1 \pm \omega_2 \gg E_J\eta_1\eta_2$, the fast oscillating terms including the following factors $\exp[\pm\mathrm{i}(\omega_1 \pm \omega_2)t]$, $\exp[\pm2\mathrm{i}\omega_1t]$, $\exp[\pm2\mathrm{i}\omega_2t]$ can be dropped for their influences are averaged out in the long run. Fortunately, for parameters listed in our paper, such requirements are fulfilled. Thus, the effec-

tive Hamiltonian is

$$H = \omega_1 a_1^+ a_1 + \omega_2 a_2^+ a_2 + E_J \sum_j \left\{1 - \frac{1}{2}[\eta_1^2 (2a_1^+ a_1 + 1) + \eta_2^2 (2a_2^+ a_2 + 1)\right\} \sigma_j^x + \frac{e^2 C_\Sigma}{C_m^2} \sum_j \sigma_j^z \sigma_j^z, \quad \text{(b6)}$$

which is exactly eq. (10).

Notice that in the above deduction we have used Riemann-Lebesgue lemma[22]

$$\lim_{\omega\to\infty} \int_a^b f(t) e^{i\omega t} dt = \lim_{\omega\to\infty} \frac{1}{i\omega} \int_a^b f(t) de^{i\omega t} = \lim_{\omega\to\infty} \frac{1}{i\omega} \left[f(t) e^{i\omega t} \Big|_a^b - \int_a^b e^{i\omega t} df(t) \right] = 0. \quad \text{(b7)}$$

One (Ai Q.) of the authors thanks W. Y. Huo for warm discussions.

1 Osterloh A, Amico L, Falci G, et al. Scaling of entanglement close to a quantum phase transition. Nature (London), 2002, 416: 608－610[doi]

2 Gu S J, Deng S S, Li Y Q, et al. Entanglement and quantum phase transition in the extended hubbard model. Phys Rev Lett, 2004, 93: 086402[doi]

3 Sachdev A. Quantum Phase Transition. Cambridge: Cambridge University Press, 1999

4 Emary C, Brandes T. Quantum chaos triggered by precursors of a quantum phase transition: The Dicke model. Phys Rev Lett, 2003, 90: 044101[doi]

5 Li Y, Wang Z D, Sun C P. Quantum criticality in a generalized Dicke model. Phys Rev A, 2006, 74: 023815[doi]

6 Yang S, Song Z, Sun C P. Dynamic generation of entangling wave packets in XY spin system with decaying long-range couplings. Sci China Ser G-Phys Mech Astron, 2008, 51: 1677－1681

7 Si L M, Hou J X. Quantum phase transition and entanglement in Li atom system. Sci China Ser G-Phys Mech Astron, 2008, 51: 1677－1681

8 Quan H T, Song Z, Liu X F, et al. Decay of Loschmidt echo enhanced by quantum criticality. Phys Rev Lett, 2006, 96: 160604

9 Peres A. Quantum Theory: Concepts and Methods. New York: Kluwer Academic Publishers, 2002

10 Wallraff A, Schuster D I, Blais A, et al. Strong coupling of a single photon to a superconducting qubit using circuit quantum electrodynamics. Nature (London), 2004, 431: 162－167[doi]

11 Chiorescu I, Bertet P, Semba K, et al. Coherent dynamics of a flux qubit coupled to a harmonic oscillator. Nature (London), 2004, 431: 159－162[doi]

12 You J Q, Nori F. Superconducting circuits and quantum information. Phys Tod, 2005, 58: 42－47

13 Wang Y D, Xue F, Song Z, et al. Detection mechanism for quantum phase transition in superconducting qubit array. Phys Rev B, 2007, 76: 174519[doi]

14 Zhang J F, Peng X H, Rajendran N, et al. Detection of quantum critical points by a probe qubit. Phys Rev Lett, 2008, 100: 100501[doi]

15 Moon K, Girvin S M. Theory of microwave parametric down-conversion and squeezing using circuit QED. Phys Rev Lett, 2005, 95: 140504[doi]

16 Scully M O, Zubairy M S. Quantum Optics. Cambridge: Cambridge University Press, 1997

17 Pfeuty P. The one-dimensional Ising model with a transverse field. Ann Phys, 1970, 57: 79－90[doi]

18 Hanbury-Brown H, Twiss R Q. A new type of interferometer for use in radio astronomy. Philos Mag, 1954, 45(366): 663－682

19 Knight P L, Allen L. Concepts of Quantum Optics. Oxford: Pergamon Press, 1983

20 Hoyos J A, Vojta T. Theory of smeared quantum phase transitions. Phys Rev Lett, 2008, 100: 240601[doi]

21 Anderson P W. Random-phase approximation in the theory of superconductivity. Phys Rev, 1958, 112: 1900－1916[doi]

22 Li J C, Zhou X C. Asymptotic Approach in Mathematic Physics. Beijing: Scientific Press, 1998